Original Article

Diagnostic performance of synthetic magnetic resonance imaging in the prognostic evaluation of rectal cancer

Lidi Ma[#], Shanshan Lian[#], Huimin Liu, Tiebao Meng, Weilong Zeng, Rui Zhong, Linchang Zhong, Chuanmiao Xie

Department of Radiology, Sun Yat-sen University Cancer Center, State Key Laboratory of Oncology in South China, Sun Yat-sen University, Guangzhou, China

Contributions: (I) Conception and design: L Ma, S Lian, H Liu; (II) Administrative support: C Xie; (III) Provision of study materials or patients: All authors; (IV) Collection and assembly of data: All authors; (V) Data analysis and interpretation: L Ma, S Lian; (VI) Manuscript writing: All authors; (VII) Final approval of manuscript: All authors.

[#]These authors contributed equally to this work.

Correspondence to: Chuanmiao Xie. Department of Radiology, Sun Yat-sen University Cancer Center, State Key Laboratory of Oncology in South China, Collaborative Innovation Center for Cancer Medicine, Guangdong Key Laboratory of Nasopharyngeal Carcinoma Diagnosis and Therapy, Guangzhou 510060, China. Email: xchuanm@sysucc.org.cn.

Background: Numerous factors are related to the prognosis of rectal cancer, including T stage, N stage, metastasis, extramural venous invasion (EMVI), circumferential resection margin (CRM), and tumor differentiation. However, it is still a challenge to precisely evaluate them before therapy; therefore, we investigate whether synthetic magnetic resonance imaging and apparent diffusion coefficient (ADC) values could help predict the prognostic factors of rectal cancer.

Methods: Eighty-seven patients (55 men and 32 women; mean age, 59±11 years) with pathologically confirmed rectal cancer were enrolled. Preoperative quantitative metrics, including T1, T2, proton density (PD), and ADC values, were measured with diffusion-weighted imaging (DWI) acquired by a single-shot echo-planar sequence and synthetic magnetic resonance imaging acquired by a multi-dynamic multi-echo sequence at 3.0 T, in patients with rectal cancer by two radiologists. We evaluated the diagnostic performance of synthetic magnetic resonance imaging using the independent sample *t*-test or Mann-Whitney U test and receiver operating characteristic (ROC) curve and multivariate logistic regression analyses and compared the area under the ROC curve of quantitative values using the DeLong test.

Results: The T2 and PD values showed a significant reduction among patients with poor differentiation and lymph node metastasis in rectal cancer. The area under the ROC curve values of T2 and PD values for predicting magnetic resonance imaging N stage and differentiation were 0.734, 0.682, and 0.673, 0.686, respectively. Moreover, combining T2 and PD values for magnetic resonance imaging N stage slightly improved the area under the ROC curve value of 0.774 (95% CI, 0.673–0.876). In the present study, the ADC and T1 values were not significant in the differentiation or clinical stage of rectal cancer (RC).

Conclusions: Quantitative T2 and PD values obtained by synthetic magnetic resonance imaging might be used for evaluating prognostic factors of rectal cancer noninvasively. Furthermore, combining T2 and PD values further improved the diagnostic performance of magnetic resonance imaging N staging in rectal cancer. The ADC and T1 values were not significant in the differentiation or clinical stage of RC.

Keywords: Synthetic magnetic resonance imaging (synthetic MRI); rectal cancer; prognostic factors

Submitted Jan 10, 2022. Accepted for publication Mar 22, 2022.
doi: 10.21037/qims-22-24
View this article at: https://dx.doi.org/10.21037/qims-22-24

Introduction

Colorectal cancer is the third most common malignancy and the second leading cause of cancer-related death globally (1), of which most is adenocarcinoma, approximately accounting for 30–35% in colorectal cancer cases (2). Numerous factors are related to the prognosis of rectal adenocarcinoma, including T stage, N stage, metastasis, extramural venous invasion (EMVI), circumferential resection margin (CRM), and tumor differentiation (3). Surgery alone is suitable for patients in the T1-2N0 stage. Preoperative neoadjuvant chemoradiotherapy (nCRT) is suitable for patients with locally advanced cancer in T3-T4 or T1-2N1-2 stage, which not only decreases local recurrence rates, but also improves disease-free survival (4,5). However, nCRT may adversely affect anorectal function (6). Thus, identifying the clinical staging of rectal cancer (RC) precisely is important for treatment decisions on the benefits from neoadjuvant therapy for patients at high risk for local recurrence while avoiding excessive preoperative treatment for patients with early-stage cancer.

Although assessing the interobserver agreement and diagnostic accuracy of RC remains a challenge, high spatial resolution magnetic resonance imaging (MRI) has been a standard preoperative method for RC assessment according to the National Comprehensive Cancer Network guidelines (5,7,8) and is widely used for noninvasive localization, detection, and primary staging of RC (9,10). Conventional MRI has a limit in reflecting the biological characteristics of tumors due to the lack of objective and quantitative parameters. In recent years, many studies have indicated that multiple quantitative MRI (qMRI) techniques, including intravoxel incoherent motion, diffusion-weighted imaging (DWI), diffusion kurtosis imaging (DKI), and dynamic contrast-enhanced imaging, potentially predict the risk factors of RC (11-14). However, the overlap of apparent diffusion coefficient (ADC) values in some subgroups, the long acquisition time of conventional technologies, complex postprocessing and analysis methods, and insufficient standardized image acquisition protocols have limited their clinical application. Therefore, it is necessary to identify a fast, standardized, and robust technique.

Recently, synthetic MRI (SyMRI), a novel qMRI with a multidynamic multiecho (MDME) sequence, has been recommended for clinical work. Compared with conventional MRI, it can simultaneously quantify longitudinal relaxation time (T1), transverse relaxation time (T2), and proton density (PD) maps in a single scan within a short examination time (15). As basic intrinsic properties of MRI physics, quantitative T1, T2, and PD values can reflect the flow water content and cellular density in different tissues or assess diffuse myocardial fibrosis (16). This technique has been successfully applied in different diseases, such as differentiating benign and malignant lesions in breast or prostate cancer and facilitating grading and staging of cervical cancer. Moreover, it has shown favorable results in various central nervous system diseases (17-20) and excellent correlation with conventional mapping techniques and does not demonstrate more inferior image quality than conventional contrast-weighted images (21). One study suggested that SyMRI-derived histogram parameters of the primary tumor are associated with LN metastasis in rectal cancer but other textural features were not included (22). Zhao *et al.* (23) also reported that T2 and T1 values were important for differentiating T and N stages in RC. Nevertheless, the clinical significance of SyMRI PD values in RC remains unclear, and CRM was not included in the study. This study aimed to explore the quantitative parameters derived from SyMRI clinical stage according to the "DISTANCE" criteria (8) and RC differentiation. We present the following article in accordance with the STARD reporting checklist (available at https://qims.amegroups.com/article/view/10.21037/qims-22-24/rc).

Methods

Patients

The study was conducted in accordance with the Declaration of Helsinki (as revised in 2013). This prospective, single-center study was approved by our institutional review board, and written informed consent was obtained from each participant. From January 22, 2019, to August 16, 2021, 156 patients with suspicious rectal adenocarcinoma were recruited consecutively in our hospital. The inclusion criteria were as follows: (I) confirmed histopathological diagnosis of rectal adenocarcinoma through surgically resected specimens or endoscopic biopsy; (II) patients who underwent MRI scanning, including SyMRI and DWI, before neoadjuvant therapy or surgical resection. The exclusion criteria were as follows: (I) absence of confirmed pathological results or confirmed histopathological diagnosis of mucinous carcinomas; (II) patients who underwent radiation or neoadjuvant chemotherapy and radiation therapy before MRI; (III) absence of complete clinical data; (IV) presence of insufficient imaging quality that inadequately depicted the lesion. Finally, we enrolled 87 patients in the study (*Figure 1*).

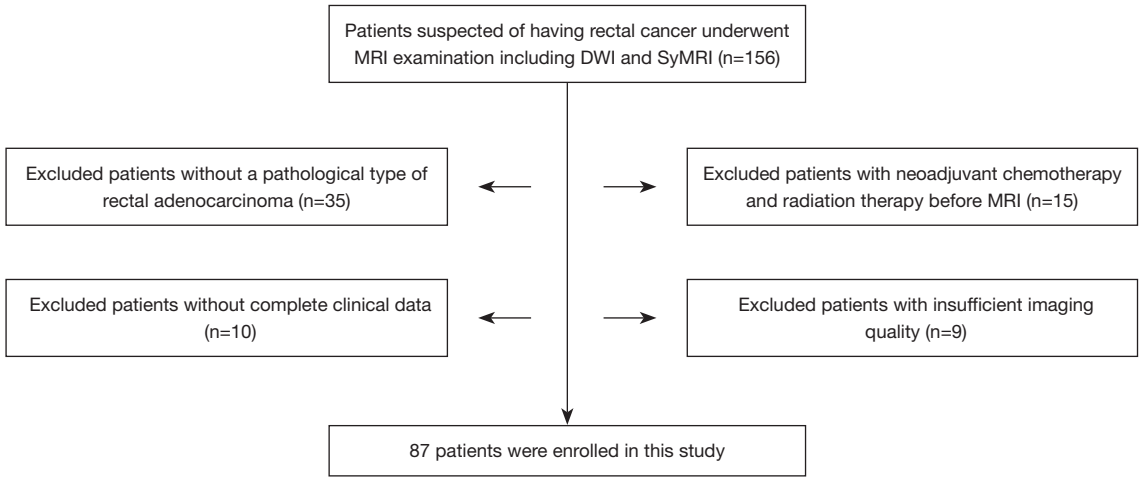

Figure 1 Flowchart of participants eligible for analysis. MRI, magnetic resonance imaging; SyMRI, synthetic magnetic resonance imaging; DWI, diffusion-weighted imaging.

Table 1 Details of MRI parameters

Parameters	AX T1WI	AX T2WI	OSag T2WI	OCor T2WI	DWI (b value of 0 and 800 s/mm^2)	MAGIC
Repetition time/echo time, ms	478/9.9	3,163/75.4	2,233/85.7	2,719/85	4,000/59.5	4,000/16.2/89.4
Slice thickness, mm	5	5	3	3	5	5
Spacing, mm	1	1	0.5	1	1	1
Field of view, cm	38	38	0.5	20	38	38
Acquisition matrix	384×288	384×384	320×320	320×288	128×128	320×256
Number of excitations [NEX]	2	2	2.5	1	6	1
Scan time, min:s	2:03	2:13	1:57	1:52	1:48	4:32

MRI, magnetic resonance imaging; AX T1W1, axial T1-weighted image; AX T2W2, axial T2-weighted image; OCor, oblique coronal; OSag, oblique sagittal; DWI, diffusion-weighted imaging; NEX, number of excitations; MAGIC, magnetic resonance image compilation.

Magnetic resonance image acquisition

All MRI examinations were performed on a 3.0 T scanner (Signa Pioneer, GE Healthcare), and a 32-channel phased-array body coil was used. We added a SyMRI sequence into the routine clinical magnetic resonance examination. The conventional MRI protocols in our hospital include the following sequence: oblique axial T1-weighted imaging and sagittal, oblique axial, and oblique coronal T2-weighted imaging, and DWI (b values of 0 and 800 s/mm^2). For SyMRI, a 2D fast spin-echo (FSE) MDME sequence included two echo times (16.2/89.4 ms) and four automatically calculated saturation delay times. The detailed parameters are summarized in *Table 1*. The total scan time for SyMRI was 4 min and 32 s. We loaded the MDME sequence into SyMRI 7.2 (SyntheticMR, Linköping, Sweden) for postprocessing, generating quantitative T1, T2, and PD maps within 10 s. Subsequently, we generated ADC maps from the DWI images on the scanner console.

Imaging analysis

For SyMRI-derived parameters, the region of interest (ROI) was manually delineated on the slice with the largest tumor diameter on synthetic T2-weighted image without artifacts, avoiding margins and the intestinal lumen, by two radiologists (readers 1 and 2, respectively having 10 and 3 years of experience in rectal imaging), and was then transferred to the T1 and PD maps. For the ADC value, we delineated a ROI on the ADC map along the border of the tumor on the slice with the largest tumor diameter in reference to the corresponding synthetic T2-weighted

Table 2 Clinical characteristics

Characteristics	Number of patients
Age (years) (mean ± SD)	59±11
Sex	
Male	55
Female	32
CEA level (ng/mL), median (Q1, Q3)	5.24 (2.54–10.55)
mrT stage	
T1–T2	22
T3–T4	65
mrN stage	
N0	30
N1–N2	57
mrEMVI	
Absent	65
Present	22
mrCRM	
Absent	57
Present	30
Differentiation	
Well/moderate	71
Poor	16
Surgery	18
nCRT	69

CEA, carcinoembryonic antigen; mrEMVI, magnetic resonance extramural venous invasion; mrCRM, magnetic resonance circumferential resection margin; nCRT, neoadjuvant chemoradiotherapy.

image without susceptibility artifacts. The mean T1, T2, PD, and ADC values were automatically calculated in the ROIs for each participant. The final data were reviewed by reader 3, a senior radiologist with >30 years of experience in rectal imaging. When ambiguous cases were considered by the senior radiologist or big discrepancy of the values, consensus was obtained following discussion. The average values of the two radiologists were used for analysis.

MR images were assessed by readers 1 and 2, knowing nothing about other materials except for the image information. Image evaluation features according to the "DISTANCE" criteria (8) mainly were as follows: distance from the inferior part of the tumor to the transitional skin, T staging, anal complex—sphincters and puborectal muscles, nodal staging, CRM, and EMVI. Reader 3 reviewed the assessment from the two radiologists. The consensus was obtained following the discussion when dealing with ambiguous cases by the senior radiologist. Finally, T stage, N stage, EMVI, and CRM were included for analysis.

Pathological analysis

For patients undergoing surgical resection, we collected the pathological characteristics including differentiation, pathological T stage, N stage, perineural invasion, and EMVI, which were assessed according to the eighth edition of the American Joint Committee on Cancer tumor-node-metastasis staging system. For patients receiving nCRT, differentiation of endoscopic biopsy was collected.

Statistical analyses

Statistical analyses were performed using SPSS (version 25.0, IBM) and MedCalc statistical software (version 20.011). The differences in T1, T2, PD, and ADC values were assessed using the independent sample *t*-test or Mann-Whitney U test according to the normality test and homoscedasticity of data in each subgroup for the following groups: mrT1–2 and mrT3–4, mrN0, and mrN1–2, EMVI, CRM, and differentiation. Interobserver variability of quantitative map parameters was evaluated through the interclass correlation coefficient (ICC) according to the following criteria: <0.40, 0.40–0.59, 0.60–0.74, 0.75–1.00, representing poor, fair, good and excellent, respectively. The receiver operating characteristic (ROC) curve was plotted to assess the performance of quantitative values. The optimal cut-off values were determined by the Youden index; the area under the ROC curve (AUC), sensitivity, and specificity were calculated. Moreover, we evaluated the diagnostic performance of the combined parameters by multivariate logistic regression analysis, comparing the performance of ROC curves by the DeLong test. Differences of two-tailed P values <0.05 were considered statistically significant.

Results

Patient characteristics

In total, we enrolled 87 patients [55 (63.2%) men and 32 (36.8%) women, mean age, 59±11 years] according to the selection criteria. The baseline characteristics of these patients are shown in *Table 2*.

Table 3 T1, T2, PD, and ADC values among different subgroup

Groups	T1 (ms)	T2 (ms)	PD (pu)	ADC (10^{-6} mm^2/s)
mrT stage				
T1–T2	1,353 (1,278–1,461)	84.05±5.72	79 [76–81]	1,300 (1,180–1,370)
T3–T4	1,346 (1,268–1,417)	83.80±4.48	79 (74–83.8)	1,245 (1,142–1,368)
P value	0.703	0.669	0.554	0.879
mrN stage				
N0	1,371 (1,265–1,446)	86.67±4.18	82.07±5.05	1250 (1180–1440)
N1–N2	1,337 (1,277–1,412)	82.50±4.44	76.96±6.72	1270 (1150–1340)
P value	0.968	<0.001	0.012	0.701
mrEMVI				
Absent	1,337 (1,266–1,422)	83.77±4.63	78.75±6.75	1,260 (1,135–1,350)
Present	1,372 (1,295–1,420)	84.09±5.19	78.27±6.48	1,255 (1,195–1,370)
P value	0.42	0.866	0.925	0.646
mrCRM				
Absent	1,353.5 (1,265–1,431)	84.07±4.93	79 (76–83.25)	1,265 (1,148–1,370)
Present	1,332 (1,285–1,403.5)	83.45±4.46	78 (73–80.5)	1,240 (1,165–1,365)
P value	0.957	0.529	0.600	0.947
Differentiation				
Well/moderate	1,363 (1,278–1,438)	84.38±4.43	79 [76–84]	1,250 (1,157–1,370)
Poor	1,297 (1,265–1,409)	81.47±5.59	76 [72–80]	1,290 (1,150–1,360)
P value	0.193	0.017	0.036	0.711

Continuous quantitative variables as mean ± standard deviation or median (first quartile and third quartile). PD, proton density; ADC, apparent diffusion coefficient; mrEMVI, magnetic resonance extramural venous invasion; mrCRM, magnetic resonance circumferential resection margin.

Evaluating quantitative relaxation maps in rectal cancer subgroups

Interobserver agreement was excellent between two radiologists for the measurement of quantitative parameters. The ICCs of the T1, T2, PD, and ADC values were 0.888 [95% confidence interval (CI), 84.1–92.1%], 0.946 (95% CI, 92.3–96.2%), 0.949 (95% CI, 92.7–96.4%), and 0.891 (95% CI, 84.5–92.4%), respectively.

The differences between subgroups and quantitative parameters in terms of T1, T2, PD, and ADC values are summarized in *Table 3*. We expressed continuous quantitative variables as mean ± standard deviation or median (first quartile and third quartile) according to each subgroup's normality test and homoscedasticity of data. The mean T2 and PD values of poor differentiation were significantly lower than well or moderate differentiation {T2, 81.47±5.59 *vs.* 84.38±4.43 ms; PD, 76 [72–80] *vs.* 79 [76–84] pu; P=0.017, 0.036, respectively}. Additionally, the mean T2 and PD values of tumors with nodal involvement (mrN1–2) were also significantly lower than in tumors without metastatic lymph nodes (mrN0) (T2, 82.50±4.44 *vs.* 86.67±4.18 ms; PD, 76.96±6.72 *vs.* 82.07±5.05 pu). From the optimal cutoff values, when T2 value ≤79.75 ms or PD value ≤73.5 pu, rectal cancer is more likely to be poorly differentiated. Also rectal cancer is more likely to have lymph node metastases when T2 value ≤86.25 ms or PD value ≤76.5 pu. The T2 and PD values were not significantly different in other subgroups in terms of T stage, EMVI, and CRM (T2, P=0.669, 0.866, 0.529; PD, P=0.554, 0.925, 0.600, respectively), nor were the T1 and ADC values among subgroups (*Table 3*, P>0.05). The comparison of T2 and PD values in two mrN stage and differentiation subgroups is demonstrated in *Figure 2*. Representative SyMRI images are shown in *Figures 3-5*.

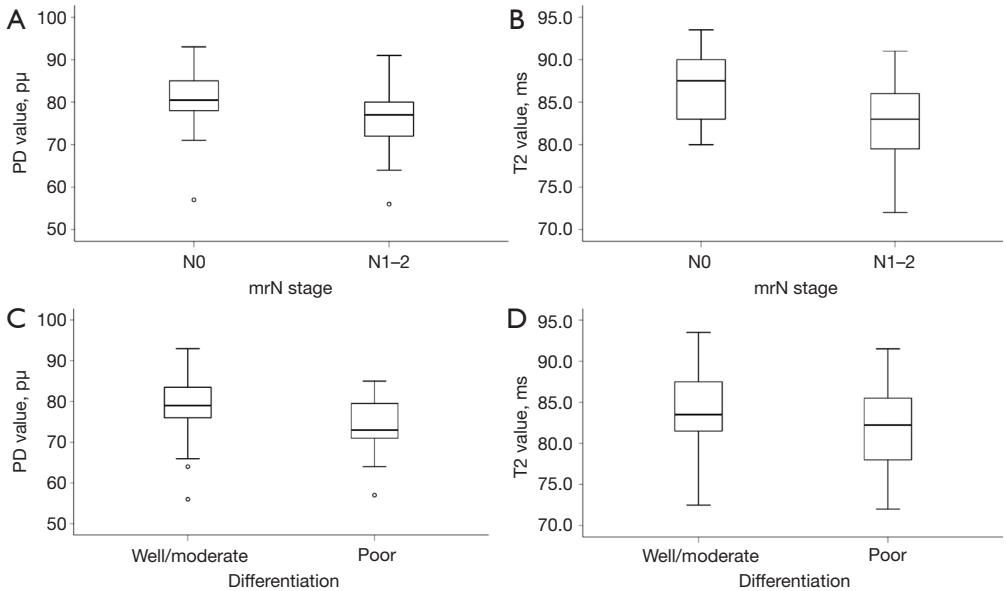

Figure 2 The comparison of T2 and PD values in two mrN stage and differentiation subgroups. (A) The box plot showing the mean PD value in mrN stage (the vertical coordinate represents PD value, the horizontal coordinate represents mrN stage). (B) The box plot showing the mean T2 value in mrN stage (the vertical coordinate represents T2 value, the horizontal coordinate represents mrN stage). (C) The box plot showing the mean PD value in differentiation (the vertical coordinate represents PD value, the horizontal coordinate represents differentiation). (D) The box plot showing the mean T2 value in differentiation (the vertical coordinate represents T2 value, the horizontal coordinate represents differentiation). The mean PD and T2 values of mrN1–2 and poor differentiation were significantly lower than mrN0 and well or moderate differentiation (all $P<0.05$). PD, proton density; mr, magnetic resonance.

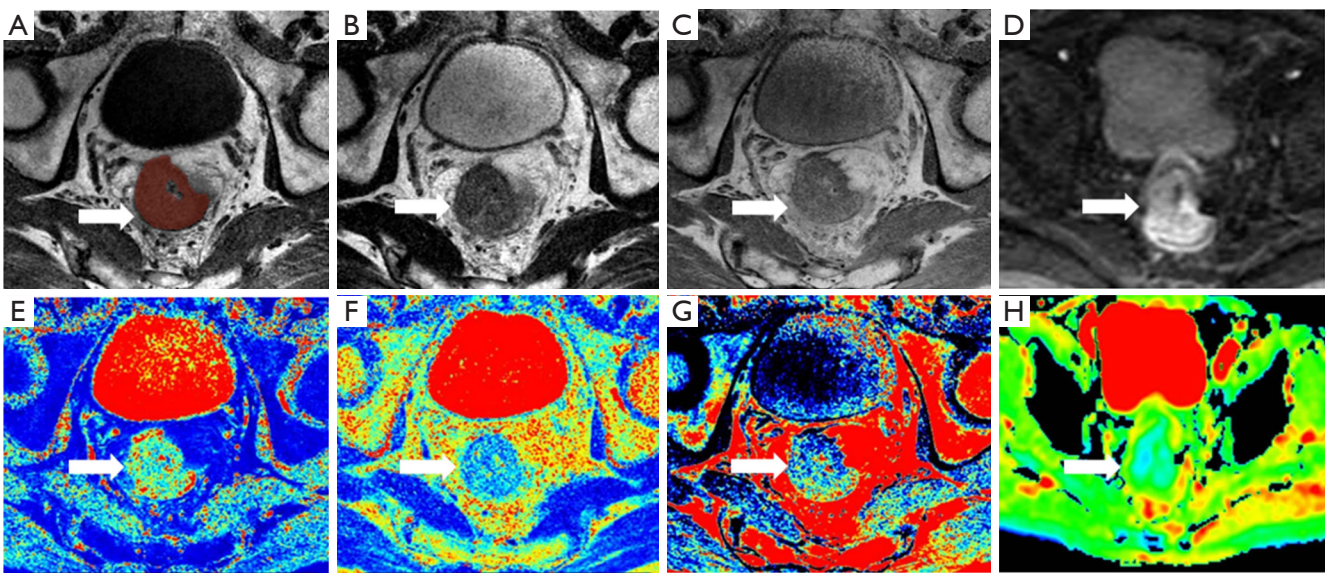

Figure 3 A 71-year-old man with moderate differentiation RC [T3N0, mesorectal fascia (–), extramural venous invasion (–)]. (A-C) synthetic T1-, T2-, and PD-weighted images, respectively; (D) axial DWI (b=800 s/mm^2); (E-G) T1, T2, and PD maps derived from SyMRI indicating the mean T1, T2, and PD values, which were drawn along the contour of the tumor on the slice with the largest tumor diameter were 1,174 ms, 82 ms, and 78 pu, respectively. (H) ADC map indicates that the mean ADC value was 1,070×10^{-6} mm^2/s. The arrow points to the tumor. RC, rectal cancer; DWI, diffusion-weighted imaging; ADC, apparent diffusion coefficient; PD, proton density; SyMRI, synthetic magnetic resonance imaging.

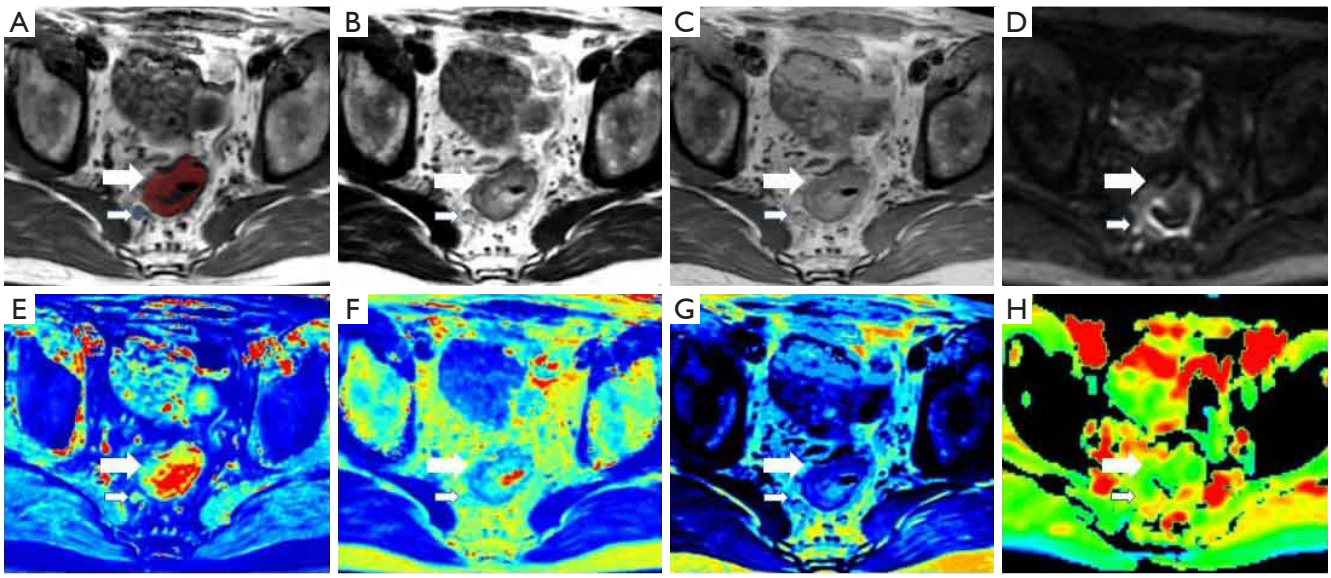

Figure 4 A 48-year-old man with moderate differentiation RC [T3N2, mesorectal fascia (–), extramural venous invasion (+)]. (A-C) synthetic T1-, T2-, and PD-weighted images, respectively; (D) axial DWI (b=800 s/mm^2); (E-G) T1, T2, and PD maps derived from SyMRI indicating the mean T1, T2, and PD values, which were drawn along the contour of the tumor on the slice with the largest tumor diameter were 1,284 ms, 80 ms, and 72 pu, respectively. (H) ADC map indicates that the mean ADC value was 1,595×10^{-6} mm^2/s. The small arrow points to the metastatic lymph node; the large arrow points to the tumor. RC, rectal cancer; PD, proton density; DWI, diffusion-weighted imaging; SyMRI, synthetic magnetic resonance imaging; ADC, apparent diffusion coefficient.

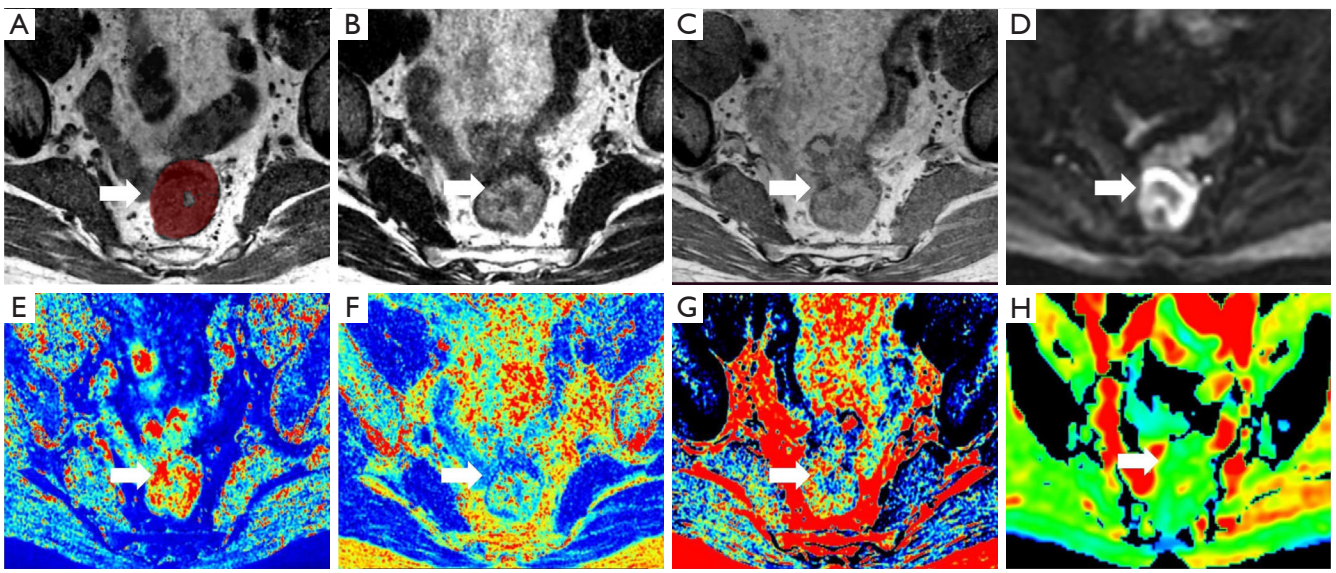

Figure 5 A 45-year-old man with poor differentiation RC [T2N0, mesorectal fascia (–), extramural venous invasion (–)]. (A-C) synthetic T1-, T2-, and PD-weighted images, respectively; (D) axial DWI (b=800 s/mm^2); (E-G) T1, T2, and PD maps derived from SyMRI indicating the mean T1, T2, and PD values, which were drawn along the contour of the tumor on the slice with the largest tumor diameter were 1,103 ms, 72 ms, and 70 pu, respectively. (H) ADC map indicates that the mean ADC value was 1,315×10^{-6} mm^2/s. The arrow points to the tumor. RC, rectal cancer; PD, proton density; DWI, diffusion-weighted imaging; SyMRI, synthetic magnetic resonance imaging; ADC, apparent diffusion coefficient.

Table 4 Diagnostic performance of T2 and PD values in predicting the prognostic factors

Parameters	AUC (95% CI)	Sensitivity (%)	Specificity (%)	Cut-off (ms/pu)	P value
T2 value (differentiation)	0.673 (0.510–0.836)	46.7	86.7	79.75	0.036
PD value (differentiation)	0.686 (0.534–0.838)	53.3	81.7	73.5	0.024
PD + T2 value (differentiation)	0.756 (0.600–0.911)	86.7	63.4		0.002
T2 value (mrN stage)	0.734 (0.624–0.863)	77.2	60	86.25	<0.001
PD value (mrN stage)	0.682 (0.566–0.797)	45.6	86.7	76.5	0.006
PD + T2 value (mrN stage)	0.774 (0.673–0.876)	75.4	70		<0.001

AUC, area under the receiver operating characteristic curve; PD, proton density.

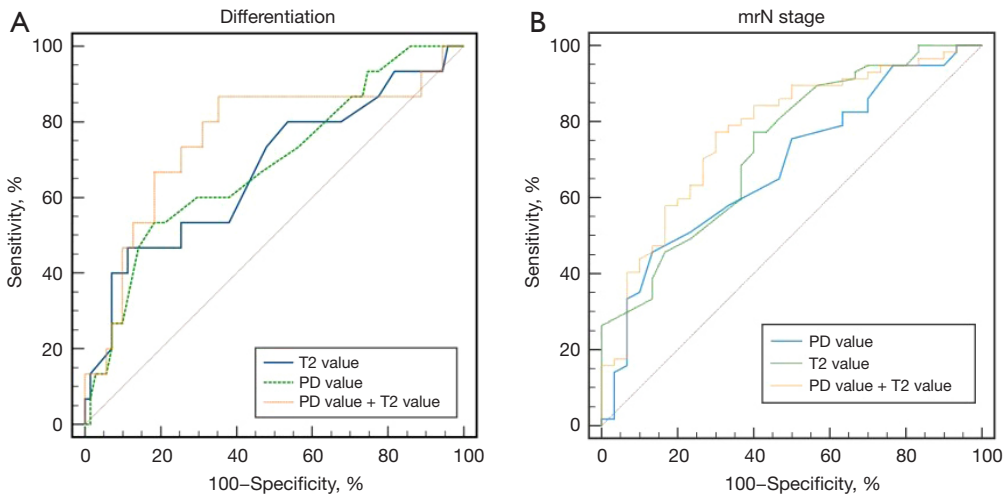

Figure 6 ROC curve analyses of T2 and PD values and model combing of the two in the field of (A) differentiation and (B) mrN stage. (A) The AUC values of T2, PD and combined of them for well or moderate differentiation and poor differentiation were 0.673, 0.686 and 0.756, respectively. (B) The AUC values of T2 and PD values for mrN0 and mrN1–2 were 0.734 and 0.682, respectively; and the AUC value of the combination of T2 + PD for mrN stage was 0.774, which showed that the combined indicator performance was better than PD values individually. mr, magnetic resonance; ROC, receiver operating characteristic; PD, proton density; AUC, area under the receiver operating characteristic curve.

ROC curve analysis

Table 4 and *Figure 6* show the ROC analysis of the T2 and PD values in predicting mrN stage and RC differentiation. The AUC values of T2 and PD for well or moderate differentiation and poor differentiation were 0.673 (95% CI, 0.510–0.836) and 0.686 (95% CI, 0.534–0.838), respectively. The AUC values of T2 and PD values for mrN0 and mrN1–2 were 0.734 (95% CI, 0.624–0.863) and 0.682 (95% CI, 0.566–0.797), respectively. The optimal cut-off values for T2 and PD to differentiate between well or moderate and poor differentiation were 79.75 ms and 73.5 pu, respectively. We calculated that the optimal cut-off values for distinguishing mrN0 and mrN1–2 were 86.25 ms and 76.5 pu for T2 and PD, respectively. Combining T2 and PD values significantly improved the diagnostic performance in distinguishing mrN stage. The AUC value of the combination of T2 + PD for mrN stage was 0.774 (95% CI, 0.673–0.876), which showed that the combined indicator performance was better than PD values individually. The non-significant differences were as follows: mrN stage, T2 *vs.* PD, P=0.52; T2 + PD *vs.* PD, P=0.05; T2 + PD *vs.* T2, P=0.39. The AUC value of combining T2 and PD values for differentiation was 0.756 (95% CI, 0.600–0.911), which did not improve the

diagnostic performance (T2 + PD *vs.* T2, P=0.12; T2 + PD *vs.* PD, P=0.23). Overall, the combined model of T2 and PD values performed well for mrN stage but was not significant for differentiation.

Discussion

Our study investigated whether the histological differentiation and clinical stage of rectal adenocarcinoma can be evaluated by quantitative SyMRI-derived maps and ADC value before therapy. The clinical stage of patients with neoadjuvant chemotherapy was determined by our team according to the certain imaging findings specified in 2017 European Society for Medical Oncology (ESMO) Clinical Practice Guidelines (3). For participants receiving neoadjuvant treatment, routine MRI was repeated after completed treatment to further assess response. The results demonstrated that T2 and PD values had good diagnostic efficacy in tumor differentiation and mrN stage.

The T2 and PD values were significantly lower in poor differentiation and mrN1–2 than in well or moderate differentiation and mrN0. We found no significant difference between T1 and ADC values in each subgroup.

The poorer the tumor differentiation or positive lymph node metastasis, the lower the PD value in RC. Gland formation with tumor cells and obvious atypia in high-grade tumors, but also nuclear polymorphism, increased cell density, and micronecrosis contribute to a decreased PD value. To date, several studies have confirmed the potential of the PD value for the diagnosis and grading of prostate, bladder, and breast cancers (16,20,24), consistent with our result. However, Zhao *et al.* (23) reported a different result; they compared the PD values of pathological staging by SyMR at 3T and found no significant differences. The small sample size and the unbalanced data distribution may contribute to the different results.

In this study, the mean T2 value of poor differentiation was significantly lower than that of well or moderate differentiation in RC. Additionally, we discovered the T2 value in patients with RC with mrN stage 1–2 was significantly lower than in those with mrN stage 0, with a cut-off value of 86.25 ms. The quantitative T2 relaxation time is widely used in the brain, breast, kidney, and prostate (16,25-27). The R2* value was also closely related to histopathological prognostic factors in RC by T2*-weighted imaging (28), which was consistent with the present result. Previous results on the association between T2 value and prognosis factors in other diseases have been consistent (24,27,29). For example, Li *et al.* (18) found that the accelerated T2 mapping sequence by SyMRI can facilitate grading and staging of cervical cancer.

Decreased T2 value in highly aggressive RC reflects the reduction of the free water content in the extracellular fluid space and tissues. There are many factors involved in the above results, including the presence of increased cell density, nuclear-to-cytoplasmic ratios, and nuclear polymorphism (30). Therefore, we can assume that T2 and PD values may reflect microstructural characteristics of various neoplastic tumors or tissues. Low T2 and PD values in patients may reflect intermediate or advanced RC, which are advantageous to prognosis prediction and establishment of treatment strategies.

As an effective tool, the T1 value can evaluate diffuse myocardial fibrosis noninvasively and even predict poor prognosis (31). Meng *et al.* (32) showed satisfactory performance in distinguishing nasopharyngeal carcinoma and benign hyperplasia in the nasopharynx. Nevertheless, T1 values showed no significant differences in each subgroup of prognosis factors for RC in the present study, consistent with Cui *et al.*'s (16) result on the diagnosis and grading of prostate cancer. The differences in tumor types or ROI delineation methods may contribute to the discrepancy.

Despite the improved detection ability of conventional DWI in tumor or lymph nodes in the mesorectum, the value of ADC in clinical practice remains controversial (33,34). In the present study, the ADC value was not significant in the differentiation or clinical stage of RC. Akashi *et al.* (35) reported a similar result. Notably, any parameters, including T1, T2, PD values derived from SyMRI or ADC values, were not significant for mrT stage, EMVI, or CRM in RC. A small patient population and differences in the inclusion or selection of cases or subgroups in the study might be the reasons for the lack of statistical significance. Thus, in the future, we need larger populations to investigate the actual values of SyMRI in predicting the correlation between these parameters and RC stages.

Previous studies have confirmed that the degree of differentiation in rectal cancer is significantly associated with lymph node metastasis (36-38). The poorer differentiation, the high positive lymph node. The reasons for this way may be that poorly differentiated or undifferentiated carcinomas have a strong ability to invade the surrounding tissues, especially the lymphatic vessels. What's more, our result that the lower T2 and PD values were significantly lower in poor differentiation and mrN1–2 than in well or moderate differentiation and mrN0 is consistent with these studies.

This study has some limitations. First, this prospective study has a relatively small population in one institution. As mentioned above, sampling errors may cause deviations in the results. Further studies with a larger population are required to investigate the robustness and relevance of SyMRI in RC. Second, because most of the patients in this study received neoadjuvant chemoradiotherapy (nCRT), the pathological results could not be obtained before treatment. Although the determination of N stage is based on the MRI features recommended by the guidelines, mrN stage is not yet the gold standard, thus inevitably causing false positives or false positives with biased results. What is more, patients with T1-2 stage will undergo direct surgical resection to obtain pathology; most patients with T3 stage or lymph node metastasis suspected will undergo neoadjuvant therapy, and pathological results cannot be obtained before treatment. It may weaken the statistical results. We will expand the sample size in the follow-up study. A separate study of the relationship between pathologically confirmed lymph node status and imaging parameters. While there is a significant difference in the mean for T2 and PD in mrN stage and differentiation, it is difficult to exclude the possibility of overlapping between T2 and PD parameters, which may make the test less useful in clinical practice. Finally, we only explored the correlation between SyMRI parameters and prognostic factors. In the future, we aim to assess the diagnostic performance of quantitative SyMRI parameters in predicting the complete clinical response and potentially in predicting a sustained complete clinical response in patients with RC receiving nCRT.

Conclusions

Our preliminary study demonstrated that quantitative T2 and PD values derived from SyMRI might be used for evaluating prognostic factors of RC noninvasively. Furthermore, combining T2 and PD values further improved the diagnostic performance of mrN staging in RC. The ADC and T1 values were not significant in the differentiation or clinical stage of RC in the present study.

Acknowledgments

We would like to thank Editage (www.editage.com) for English language editing.
Funding: None.

Footnote

Reporting Checklist: The authors have completed the STARD reporting checklist. Available at https://qims.amegroups.com/article/view/10.21037/qims-22-24/rc

Conflicts of Interest: All authors have completed the ICMJE uniform disclosure form (available at https://qims.amegroups.com/article/view/10.21037/qims-22-24/coif). The authors have no conflicts of interest to declare.

Ethical Statement: The authors are accountable for all aspects of the work in ensuring that questions related to the accuracy or integrity of any part of the work are appropriately investigated and resolved. The study was conducted in accordance with the Declaration of Helsinki (as revised in 2013). The study was approved by the institutional review board of Sun Yat-sen University Cancer Center and informed consent was taken from all individual participants.

References

1. Sung H, Ferlay J, Siegel RL, Laversanne M, Soerjomataram I, Jemal A, Bray F. Global Cancer Statistics 2020: GLOBOCAN Estimates of Incidence and Mortality Worldwide for 36 Cancers in 185 Countries. CA Cancer J Clin 2021;71:209-49.
2. Siegel RL, Miller KD, Jemal A. Cancer statistics, 2020. CA Cancer J Clin 2020;70:7-30.
3. Glynne-Jones R, Wyrwicz L, Tiret E, Brown G, Rödel C, Cervantes A, Arnold D; ESMO Guidelines Committee. Rectal cancer: ESMO Clinical Practice Guidelines for diagnosis, treatment and follow-up. Ann Oncol 2017;28:iv22-40.
4. Sebag-Montefiore D, Stephens RJ, Steele R, Monson J, Grieve R, Khanna S, Quirke P, Couture J, de Metz C,

Myint AS, Bessell E, Griffiths G, Thompson LC, Parmar M. Preoperative radiotherapy versus selective postoperative chemoradiotherapy in patients with rectal cancer (MRC CR07 and NCIC-CTG C016): a multicentre, randomised trial. Lancet 2009;373:811-20.
5. Benson AB, Venook AP, Al-Hawary MM, Cederquist L, Chen YJ, Ciombor KK, et al. Rectal Cancer, Version 2.2018, NCCN Clinical Practice Guidelines in Oncology. J Natl Compr Canc Netw 2018;16:874-901.
6. Canda AE, Terzi C, Gorken IB, Oztop I, Sokmen S, Fuzun M. Effects of preoperative chemoradiotherapy on anal sphincter functions and quality of life in rectal cancer patients. Int J Colorectal Dis 2010;25:197-204.
7. Beets-Tan RG, Lambregts DM, Maas M, Bipat S, Barbaro B, Caseiro-Alves F, Curvo-Semedo L, Fenlon HM, Gollub MJ, Gourtsoyianni S, Halligan S, Hoeffel C, Kim SH, Laghi A, Maier A, Rafaelsen SR, Stoker J, Taylor SA, Torkzad MR, Blomqvist L. Magnetic resonance imaging for the clinical management of rectal cancer patients: recommendations from the 2012 European Society of Gastrointestinal and Abdominal Radiology (ESGAR) consensus meeting. Eur Radiol 2013;23:2522-31.
8. Nougaret S, Reinhold C, Mikhael HW, Rouanet P, Bibeau F, Brown G. The use of MR imaging in treatment planning for patients with rectal carcinoma: have you checked the "DISTANCE"? Radiology 2013;268:330-44.
9. Bhoday J, Balyasnikova S, Wale A, Brown G. How Should Imaging Direct/Orient Management of Rectal Cancer? Clin Colon Rectal Surg 2017;30:297-312.
10. Battersby NJ, Moran B, Yu S, Tekkis P, Brown G. MR imaging for rectal cancer: the role in staging the primary and response to neoadjuvant therapy. Expert Rev Gastroenterol Hepatol 2014;8:703-19.
11. Lu Z, Wang L, Xia K, Jiang H, Weng X, Jiang J, Wu M. Prediction of Clinical Pathologic Prognostic Factors for Rectal Adenocarcinoma: Volumetric Texture Analysis Based on Apparent Diffusion Coefficient Maps. J Med Syst 2019;43:331.
12. Zhu L, Pan Z, Ma Q, Yang W, Shi H, Fu C, Yan X, Du L, Yan F, Zhang H. Diffusion Kurtosis Imaging Study of Rectal Adenocarcinoma Associated with Histopathologic Prognostic Factors: Preliminary Findings. Radiology 2017;284:66-76.
13. Lu B, Yang X, Xiao X, Chen Y, Yan X, Yu S. Intravoxel Incoherent Motion Diffusion-Weighted Imaging of Primary Rectal Carcinoma: Correlation with Histopathology. Med Sci Monit 2018;24:2429-36.
14. Yu X, Song W, Guo D, Liu H, Zhang H, He X, Song J, Zhou J, Liu X. Preoperative Prediction of Extramural Venous Invasion in Rectal Cancer: Comparison of the Diagnostic Efficacy of Radiomics Models and Quantitative Dynamic Contrast-Enhanced Magnetic Resonance Imaging. Front Oncol 2020;10:459.
15. Hagiwara A, Warntjes M, Hori M, Andica C, Nakazawa M, Kumamaru KK, Abe O, Aoki S. SyMRI of the Brain: Rapid Quantification of Relaxation Rates and Proton Density, With Synthetic MRI, Automatic Brain Segmentation, and Myelin Measurement. Invest Radiol 2017;52:647-57.
16. Cui Y, Han S, Liu M, Wu PY, Zhang W, Zhang J, Li C, Chen M. Diagnosis and Grading of Prostate Cancer by Relaxation Maps From Synthetic MRI. J Magn Reson Imaging 2020;52:552-64.
17. Arita Y, Takahara T, Yoshida S, Kwee TC, Yajima S, Ishii C, Ishii R, Okuda S, Jinzaki M, Fujii Y. Quantitative Assessment of Bone Metastasis in Prostate Cancer Using Synthetic Magnetic Resonance Imaging. Invest Radiol 2019;54:638-44.
18. Li S, Liu J, Zhang F, Yang M, Zhang Z, Liu J, Zhang Y, Hilbert T, Kober T, Cheng J, Zhu J. Novel T2 Mapping for Evaluating Cervical Cancer Features by Providing Quantitative T2 Maps and Synthetic Morphologic Images: A Preliminary Study. J Magn Reson Imaging 2020;52:1859-69.
19. Ji S, Yang D, Lee J, Choi SH, Kim H, Kang KM. Synthetic MRI: Technologies and Applications in Neuroradiology. J Magn Reson Imaging 2022;55:1013-25.
20. Gao W, Zhang S, Guo J, Wei X, Li X, Diao Y, Huang W, Yao Y, Shang A, Zhang Y, Yang Q, Chen X. Investigation of Synthetic Relaxometry and Diffusion Measures in the Differentiation of Benign and Malignant Breast Lesions as Compared to BI-RADS. J Magn Reson Imaging 2021;53:1118-27.
21. Jung Y, Gho SM, Back SN, Ha T, Kang DK, Kim TH. The feasibility of synthetic MRI in breast cancer patients: comparison of T2 relaxation time with multiecho spin echo T2 mapping method. Br J Radiol 2018. [Epub ahead of print]. doi: 10.1259/bjr.20180479.
22. Zhao L, Liang M, Shi Z, Xie L, Zhang H, Zhao X. Preoperative volumetric synthetic magnetic resonance imaging of the primary tumor for a more accurate prediction of lymph node metastasis in rectal cancer. Quant Imaging Med Surg 2021;11:1805-16.
23. Zhao L, Liang M, Xie L, Yang Y, Zhang H, Zhao X. Prediction of pathological prognostic factors of rectal cancer by relaxation maps from synthetic magnetic resonance imaging. Eur J Radiol 2021;138:109658.

24. Cai Q, Wen Z, Huang Y, Li M, Ouyang L, Ling J, Qian L, Guo Y, Wang H. Investigation of Synthetic Magnetic Resonance Imaging Applied in the Evaluation of the Tumor Grade of Bladder Cancer. J Magn Reson Imaging 2021;54:1989-97.
25. Matsuda M, Kido T, Tsuda T, Okada K, Shiraishi Y, Suekuni H, Kamei Y, Kitazawa R, Mochizuki T. Utility of synthetic MRI in predicting the Ki-67 status of oestrogen receptor-positive breast cancer: a feasibility study. Clin Radiol 2020;75:398.e1-8.
26. Lou B, Jiang Y, Li C, Wu PY, Li S, Qin B, Chen H, Wang R, Wu B, Chen M. Quantitative Analysis of Synthetic Magnetic Resonance Imaging in Alzheimer's Disease. Front Aging Neurosci 2021;13:638731.
27. Adams LC, Bressem KK, Jurmeister P, Fahlenkamp UL, Ralla B, Engel G, Hamm B, Busch J, Makowski MR. Use of quantitative T2 mapping for the assessment of renal cell carcinomas: first results. Cancer Imaging 2019;19:35.
28. Peng Y, Luo Y, Hu X, Shen Y, Hu D, Li Z, Kamel I. Quantitative T2*-Weighted Imaging and Reduced Field-of-View Diffusion-Weighted Imaging of Rectal Cancer: Correlation of R2* and Apparent Diffusion Coefficient With Histopathological Prognostic Factors. Front Oncol 2021;11:670156.
29. Li Q, Xiao Q, Yang M, Chai Q, Huang Y, Wu PY, Niu Q, Gu Y. Histogram analysis of quantitative parameters from synthetic MRI: Correlations with prognostic factors and molecular subtypes in invasive ductal breast cancer. Eur J Radiol 2021;139:109697.
30. Oh J, Cha S, Aiken AH, Han ET, Crane JC, Stainsby JA, Wright GA, Dillon WP, Nelson SJ. Quantitative apparent diffusion coefficients and T2 relaxation times in characterizing contrast enhancing brain tumors and regions of peritumoral edema. J Magn Reson Imaging 2005;21:701-8.
31. Puntmann VO, Carr-White G, Jabbour A, Yu CY, Gebker R, Kelle S, Hinojar R, Doltra A, Varma N, Child N, Rogers T, Suna G, Arroyo Ucar E, Goodman B, Khan S, Dabir D, Herrmann E, Zeiher AM, Nagel E; International T1 Multicentre CMR Outcome Study. T1-Mapping and Outcome in Nonischemic Cardiomyopathy: All-Cause Mortality and Heart Failure. JACC Cardiovasc Imaging 2016;9:40-50.
32. Meng T, He H, Liu H, Lv X, Huang C, Zhong L, Liu K, Qian L, Ke L, Xie C. Investigation of the feasibility of synthetic MRI in the differential diagnosis of non-keratinising nasopharyngeal carcinoma and benign hyperplasia using different contoured methods for delineation of the region of interest. Clin Radiol 2021;76:238.e9-238.e15.
33. Heijnen LA, Lambregts DM, Mondal D, Martens MH, Riedl RG, Beets GL, Beets-Tan RG. Diffusion-weighted MR imaging in primary rectal cancer staging demonstrates but does not characterise lymph nodes. Eur Radiol 2013;23:3354-60.
34. Cho EY, Kim SH, Yoon JH, Lee Y, Lim YJ, Kim SJ, Baek HJ, Eun CK. Apparent diffusion coefficient for discriminating metastatic from non-metastatic lymph nodes in primary rectal cancer. Eur J Radiol 2013;82:e662-8.
35. Akashi M, Nakahusa Y, Yakabe T, Egashira Y, Koga Y, Sumi K, Noshiro H, Irie H, Tokunaga O, Miyazaki K. Assessment of aggressiveness of rectal cancer using 3-T MRI: correlation between the apparent diffusion coefficient as a potential imaging biomarker and histologic prognostic factors. Acta Radiol 2014;55:524-31.
36. Mo S, Zhou Z, Dai W, Xiang W, Han L, Zhang L, Wang R, Cai S, Li Q, Cai G. Development and external validation of a predictive scoring system associated with metastasis of T1-2 colorectal tumors to lymph nodes. Clin Transl Med 2020;10:275-87.
37. Japanese Society for Cancer of the Colon and Rectum. Japanese Classification of Colorectal, Appendiceal, and Anal Carcinoma: the 3d English Edition Secondary Publication. J Anus Rectum Colon 2019;3:175-95.
38. Sun ZQ, Ma S, Zhou QB, Yang SX, Chang Y, Zeng XY, Ren WG, Han FH, Xie X, Zeng FY, Sun XT, Wang GX, Li Z, Zhang ZY, Song JM, Liu JB, Yuan WT. Prognostic value of lymph node metastasis in patients with T1-stage colorectal cancer from multiple centers in China. World J Gastroenterol 2017;23:8582-90.

Cite this article as: Ma L, Lian S, Liu H, Meng T, Zeng W, Zhong R, Zhong L, Xie C. Diagnostic performance of synthetic magnetic resonance imaging in the prognostic evaluation of rectal cancer. Quant Imaging Med Surg 2022;12(7):3580-3591. doi: 10.21037/qims-22-24

